# Accepted Manuscript

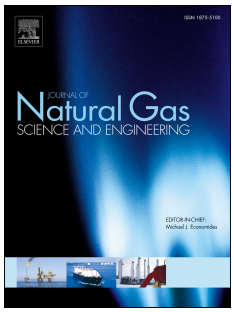


Characterization of coal fines generation: A micro-scale investigation

Tianhang Bai, Zhongwei Chen, Saiied M. Aminossadati, Zhejun Pan, Jishan Liu, Ling Li

PII: S1875-5100(15)30176-1

DOI: 10.1016/j.jngse.2015.09.043

Reference: JNGSE 1025

To appear in: *Journal of Natural Gas Science and Engineering*

Received Date: 14 July 2015

Revised Date: 10 September 2015

Accepted Date: 17 September 2015

Please cite this article as: Bai, T., Chen, Z., Aminossadati, S.M., Pan, Z., Liu, J., Li, L., Characterization of coal fines generation: A micro-scale investigation, *Journal of Natural Gas Science & Engineering* (2015), doi: 10.1016/j.jngse.2015.09.043.

# CHARACTERIZATION OF COAL FINES GENERATION: A MICRO-SCALE INVESTIGATION

**Tianhang Bai[1], Zhongwei Chen[1,2,*], Saiied M. Aminossadati[1], Zhejun Pan[3], Jishan Liu[4], Ling Li[5]**

[1] *School of Mechanical and Mining Engineering, the University of Queensland, QLD 4072, Australia*

[2] *State Key Laboratory for GeoMechanics and Deep Underground Engineering, China University of Mining & Technology, Jiangsu 221116, China*

[3] *CSIRO Energy Flagship, Private Bag 10, Clayton South 3169, Australia*

[4] School of Mechanical and Chemical Engineering, The University of Western Australia, 35 Stirling Highway, WA 6009, Australia

[5] *School of Civil Engineering, the University of Queensland, QLD 4072, Australia*

** Corresponding author email address: zhongwei.chen@uq.edu.au*

## ABSTRACT

Coal fines are commonly generated as by-product during coalbed methane production mainly due to the interaction of coal with inseam water flow. A portion of the created coal fines may settle and plug the coal cleats and hydraulic fractures due to the gravity and coal pore size constraint. This could result in the reduction of coal permeability and blockage of coalbed methane wells or gas drainage boreholes. Despite the increasing awareness of the importance of understanding coal fines, limited research has been carried out on the characterization of coal fines creation. This study aimed to numerically characterize the generation process of coal fines in micro-scale coal cleats. The Scanning Electron Microscopy (SEM) images for a coal sample from Bulli Seam of the Sydney Basin in Australia were obtained and analysed to determine the actual cleat geometries and the characteristics of coal fines distribution. Then a fully coupled fluid-structure numerical model was developed to identify the creation process of coal fines at micro-scale. The impact of pertinent production conditions on coal fines generation was studied, including production pressure drawdown, temperature, coal fines Young's modulus and strength. The SEM images revealed that the particle size distributions of the coal fines in the examined cleats were in the order of hundreds of nanometres to several microns. The results of the numerical studies showed the coal fines production increased with pressure build-up, and decreased with increasing coal fines strength with more sensitivity compared with pressure. Critical values for production pressure drawdown were obtained, above which failure area began to expand; threshold values were also determined, below which remarkable reduction of coal fines production was achieved. Coal cleat geometry plays an important role in determining coal fines production. It was noted that exposed microstructures, cleat elbow regions and micro-fracture tips are more likely to generate coal

fines. Based on these findings, guidance can be provided on the control of production conditions to mitigate coal fines issue, and new insight into where and how coal fines are created by inseam water flow can be achieved.

**Keywords:** Coal fines generation; microstructure characterization; coal dewatering; coalbed methane production

**Nomenclature**

| | |
|---|---|
| $a$ | mean cleat aperture [m] |
| $E$ | Young's modulus [Pa] |
| $\mathbf{E}$ | rate of strain tensor |
| $\mathbf{F}_T$ | load on solid surface induced by water |
| $\mathbf{I}$ | identity tensor |
| $l$ | effective flow length [m] |
| $\mathbf{n}$ | outward normal vector |
| $p$ | pressure [Pa] |
| $PD$ | maximum pressure difference between inlet and outlet [Pa] |
| $S$ | coal fines strength [Pa] |
| $T$ | temperature [°C] |
| $\mathbf{T}$ | deviatoric stress tensor |
| $u$ | mean flow velocity [m/s] |
| $\mathbf{u}$ | velocity field |
| $\nabla \mathbf{u}$ | velocity field derivative tensor |
| $V$ | coal fines production [$m^3$] |
| $\mu$ | dynamic viscosity [Pa·s] |
| $\rho$ | density [$kg/m^3$] |
| $\sigma_{11}$, $\sigma_{22}$, $\sigma_{33}$ | principal stresses [Pa] |
| $\sigma_{12}$, $\sigma_{23}$, $\sigma_{31}$ | shear stresses [Pa] |
| $\sigma_s$ | strength [Pa] |
| $\sigma_v$ | von Mises stress [Pa] |
| $\tau$ | stress in static fluid [Pa] in Eq. (3) |
| $\tau$ | stress in moving fluid [Pa] in Eq. (4) |

## 1 Introduction

Coal fines are small particles frequently found in coal seams (Magill et al. 2010; Marcinew and Hinkel 1990), and their sizes are usually between tens of nanometres and tens of microns (Fan et al. 2015; Wei et al. 2015; Zou et al. 2014). With respect to the components of coal fines, Massarotto et al. (2013) employed comparative quantitative X-ray diffraction (CQ-XRD) to elucidate that coal material is still the major substance, but with higher fraction of clay minerals than coal seams. The clay minerals mainly include kaolinite and illite. Some other minerals involving pyrite and calcite were also found in coal fines (Chen et al. 2009; Turner et al. 2013), and the mineral contents vary with different coal fines samples (Marcinew and Hinkel 1990).

Due to the presence of coal fines, although some of them are carried out by water or gas flow, some settle and plug the natural cleats, hydraulic fractures and even pumps because of the gravity and constraints of pore size or coal microstructures (Huang et al. 2012; Wang and Lan 2012). This may result in a remarkable reduction of coal reservoir permeability, and even blockage in coalbed methane wells or gas drainage boreholes. This can be considered as one of the reasons for significant reduction of coalbed methane production or gas drainage efficiency that in turn causes delays in the subsequent mining operations (Black 2011; Li et al. 2010; Magill et al. 2010; Narah 2007; Okotie and Moore 2010; Palmer et al. 2005; Zhang et al. 2011; Zou et al. 2014).

Although Massarotto et al. (2013) proposed that a portion of coal fines are suspected to be from overburden or interburden, it is generally considered that coal fines are originated from micro flow channels, namely coal cleats (Hou et al. 2014; Marcinew and Hinkel 1990). It is also suggested that coal fines are mainly produced in soft coal layers (Cao et al. 2012).

Laboratory and field studies were conducted on formation fines in porous media for oil and gas reservoir engineering (Hibbeler et al. 2003; Miranda and Underdown 1993; Muecke 1979; Nguyen et al. 2010; Qiu et al. 2008). Some research studies focused on the mechanisms of coal fines generation (Lagasca and Kovscek 2014; Liu et al. 2012; Marcinew and Hinkel 1990; Wang and Lan 2012). The common finding of earlier studies is that coal fines mainly come from inherent solid coal particles that are free in flow conduits, elastic self-regulating effect due to external pressure change, and mechanical collision induced by drilling and water flushing (Marcinew and Hinkel 1990; Wang and Lan 2012). A number of studies indicated that coal fines are mainly generated during the dewatering phase and they are produced continuously with water production (Chen et al. 2009; Hou et al. 2014; Li et al. 2010; Zhang et al. 2011). It is known that coal fines experience failure and detach from coal cleats due to high initial water production rate in the dewatering phase (Okotie and Moore 2010; Palmer et al. 2005). It is noted that coal fines can also be created during gas production (Hou et al. 2014; Magill et al. 2010). A

variety of gas and water production parameters contribute to the production of coal fines. Different impacts of varying production conditions, including production pressure drawdown, flow velocity of the carrier media and mechanical properties of coal fines, such as strength, on coal fines creation were evaluated by several researchers through laboratory and field investigations. Zou et al. (2014) performed an experiment on coal fines migration in proppant packs during dewatering process, suggesting higher flow velocity creates more coal fines, and therefore, brings more severe damage to the fracture conductivity. Cao et al. (2012) conducted an experiment on coal fines migration using varying pressure differences, concluding that higher pressure difference carries out more coal fines, and there is a critical pressure difference that initiates the migration, however they did not mention the pressure that generates coal fines. Wei et al. (2013) evaluated coal fines production by field investigation and pointed out that the well completion technology, extraction system and coal seam structure control the coal fines generation. Nevertheless, little has been done on comparing the effects of different parameters on coal fines production.

Regarding the mathematical and numerical modelling, some researchers investigated formation fines migration in porous media (Civan 2007; Khilar and Fogler 1998; Koyama et al. 2008; Mirshekari et al. 2013). Bedrikovetsky et al. (2011) developed an analytical model for strained fine particles in the petroleum engineering practices. Zeinijahromi et al. (2011) derived a mathematical model for fines migration in the petroleum field, including one-phase and two-phase flows. Wang et al. (2013) combined hydrodynamics, porous media theory and rock mechanics to develop a mathematical model for coal fines migration. Most of these studies were dealing with the problem of fines migration, while little research has been conducted with the aim of characterizing coal fines generation.

In this study, based on SEM images, fully coupled numerical simulations were developed to investigate the characteristics of coal fines generation under different production conditions with varying microstructures of coal. The scope of this study includes coal fines generated by inseam water flow during the dewatering phase. Since the dewatering process is pressure-driven, the effects of production pressure drawdown, temperature and the mechanical properties of coal fines, such as Young's modulus and strength on coal fines generation, were studied.

## 2 Governing Equations

### *2.1 Failure Criterion*

The von Mises criterion was widely used for the failure of coal (Kumar 2008; Varnes 1962; Zhu et al. 2014). This criterion was applied to investigate the failure zones in this study. Given that both the normal and shear components of the water stresses are applied on the cleat surfaces, the von Mises stress is therefore calculated as (Mises 1913):

$$\sigma_v = \sqrt{\frac{1}{2}[(\sigma_{11}-\sigma_{22})^2+(\sigma_{22}-\sigma_{33})^2+(\sigma_{33}-\sigma_{11})^2+6(\sigma_{12}^2+\sigma_{23}^2+\sigma_{31}^2)}} \quad (1)$$

where $\sigma_{11}$, $\sigma_{22}$ and $\sigma_{33}$ are principal stresses, and $\sigma_{12}$, $\sigma_{23}$ and $\sigma_{31}$ are shear stresses. Failure happens if the von Mises stress ($\sigma_v$) exceeds the strength of the material ($\sigma_s$):

$$\sigma_v > \sigma_s \quad (2)$$

*2.2 Fluid Flow*

Single water phase flow was considered in this work. For a static fluid, only isotropic normal stress acts on an element, meaning that the stress is independent of the orientation of the element surface. Therefore, the stress in the fluid at rest is (Kundu et al. 2011):

$$\tau = -p\mathbf{I} \quad (3)$$

where $p$ is the pressure, $\mathbf{I}$ is the identity tensor, which is a second-order tensor, and the negative sign denotes that the stress is compressive rather than tensile.

For a moving fluid, additional stress is developed because of viscosity, which is composed of both diagonal and off-diagonal components within $\tau$. Thus, the stress in the flowing fluid is in the form of:

$$\tau = -p\mathbf{I} + \mathbf{T} \quad (4)$$

where $\mathbf{T}$ is also called the deviatoric stress tensor. For the fluid, this symmetric tensor can be expressed as:

$$\mathbf{T} = 2\mu\mathbf{E} \quad (5)$$

where μ is the dynamic viscosity, and $\mathbf{E}$ denotes the rate of strain tensor:

$$\mathbf{E} = \frac{1}{2}(\nabla\mathbf{u}) + \frac{1}{2}(\nabla\mathbf{u})^{\mathrm{T}} \quad (6)$$

where $\mathbf{u}$ represents the velocity field, $\nabla\mathbf{u}$ means tensor derivative of the velocity field, and the superscript T symbolises the transpose of the tensor derivative.

The effect of stress on a fluid is expressed in terms of $\nabla p$ and $\nabla\mathbf{T}$, which are normal forces and viscous forces, respectively. Therefore, the water flow in coal cleat is described by the following

equations:

$$\rho\frac{\partial \mathbf{u}}{\partial t}+\rho(\mathbf{u}\cdot\nabla)\mathbf{u}=\nabla\cdot[-p\mathbf{I}+\mu(\nabla\mathbf{u}+(\nabla\mathbf{u})^{T})] \quad (7)$$

$$\nabla\cdot\mathbf{u}=0 \quad (8)$$

where $\rho$ denotes water density. The left side of Equation (7) is defined as acceleration, consisting of a time-dependent term and a convective term, which means that individual water particles experience time-dependent acceleration as well as convective acceleration. Note that the convective acceleration therein is a non-linear spatial effect. On the other hand, the right side of Equation (7) is the summation of divergence of stresses.

*2.3 Solid Deformation*

In the dewatering process, the water interacts with the solid parts, but does not dissolve such structures, and thereby, the interfaces between water and solid experience a load imposed by the water. It is the summation of pressure effect and viscous force, given by:

$$\mathbf{F}_{\mathrm{T}}=-\mathbf{n}\cdot[-p\mathbf{I}+\mu(\nabla\mathbf{u}+(\nabla\mathbf{u})^{T})] \quad (9)$$

where $\mathbf{F}_{\mathrm{T}}$ is the load exerted on solid surface by water, and **n** is the outward normal vector to the interfaces.

The commercial software COMSOL Multiphysics has been employed by many researchers to conduct numerical simulations on both fluid flow and solid mechanics (e.g., Liu et al. 2014; Vermeltfoort and Schijndel 2013). It is capable of solving the equations listed above by a time-dependent solver, using Finite Element Method (FEM). Therefore, COMSOL Multiphysics is selected as the tool to achieve the aims of this paper. In the solver, the calculations for water flow and solid deformation are performed simultaneously.

## 3 Model Implementation

*3.1 Numerical Simulation Procedure*

The numerical simulation procedure consists of six steps:

1. Determine fracture geometries from SEM images;
2. Define boundary conditions;
3. Assign properties to different parts in the simulation area;

4. Add mesh (free triangular mesh with boundary layers);
5. Run simulations; and
6. Post-process simulation results.

The procedure will be explained in detail in the following context.

*3.2 Cleat Geometry Determination*

In order to achieve the cross-section views of coal cleats and the coal fines therein, and also to obtain the same size domain to make these models comparable, four Scanning Electron Microscopy (SEM) images were taken from different regions of the sample. All images are with the same magnification at ×750. Since coal fines were considered to be mainly created from coal cleats, only the cleats and the fine particles inside were examined. The original SEM images were 157.9 µm × 118.4 µm in real size to develop the geometry of cleats with coal fines. These selected images were then implemented into MATLAB to achieve different domains that can be accepted by COMSOL Multiphysics. Several irregularly shaped, exposed microstructures and convex particles are observed (Fig. 1(a1-a4)), which are likely to become coal fines and will be examined in the following numerical studies. The size distributions of these potential fines are on the order of hundreds of nanometres to several microns, which is consistent with previous studies (Fan et al. 2015; Wei et al. 2015). Furthermore, the cleat geometries in these four images are quite different, with varying constraints, and the orientations of the cleat change at different locations.

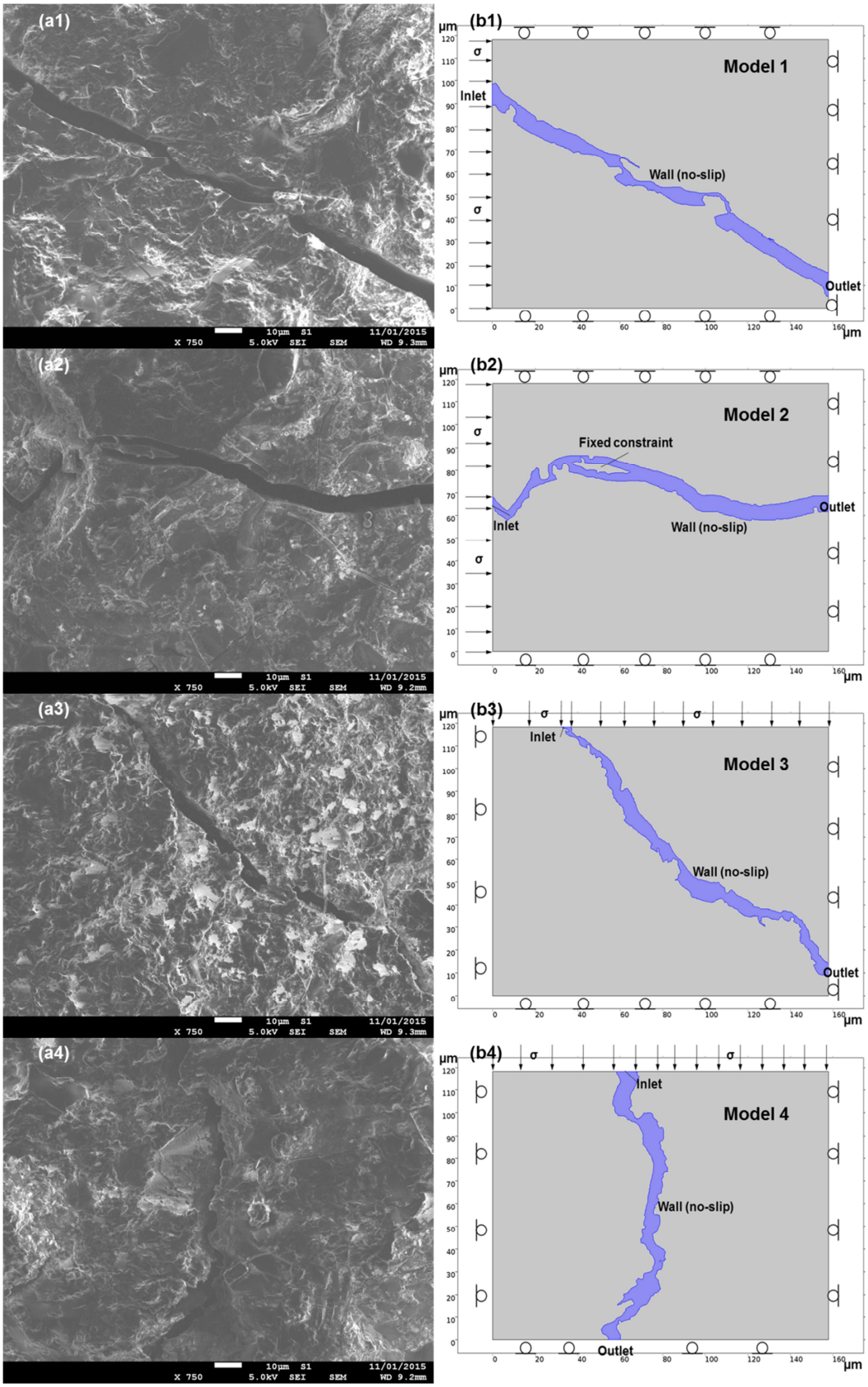


**Fig. 1.** (a) SEM images of coal cleats; (b) cleat geometries and boundary conditions used in numerical simulations.

*3.3 Model Settings*

Four numerical models were developed based on different cleat shapes as shown in Fig. 1. In these models, it was assumed that only water phase exists during the dewatering stage. According to Massaratto et al. (2013), the density of field coal fines is approximately 1800 kg/m$^3$ due to the presence of higher fraction of clay minerals like kaolinite. Most coal fines are attached to cleat surfaces with a very weak bonding force (Marcinew and Hinkel 1990); therefore, a low strength is applied. The regions, which are not in the vicinity of water flow, have little influence on coal fines output (Chen et al. 2009), and therefore in these models, the modified coal fines properties were selected as the solid parts. With respect to the physical and mechanical properties of coal fines (Greenhalgh and Emerson 1986), all values are listed in Table 1. It is noted that water density and dynamic viscosity are affected by temperature.

**Table 1** Physical and mechanical properties of the materials used in base cases of each model

| Property | Value |
|---|---|
| Density, water (kg/m$^3$) | 1000 |
| Dynamic viscosity, water (Pa·s) | 0.001 |
| Density, solid (kg/m$^3$) | 1800 |
| Young's modulus (GPa) | 5.8 |
| Poisson's ratio | 0.36 |
| Strength (Pa) | 100 |

In these models, the two-way couplings occurred on the boundaries between the water phase and the solid parts. Unlike one-way coupling which only applies the link through one direction, by employing two-way coupling method, the solid deformation is imposed by the water flow, and in turn, the water flow is influenced by the solid deformation. It should be noted that the simulation results are more accurate using two-way coupling.

The boundary conditions applied in the numerical simulations are illustrated in Fig. 1. The fluid was set to flow in a laminar regime through the coal cleats from left to right in Models 1, 2 and 3, and from top to bottom in Model 4. The numerical simulation was performed for 1.5 s. From 0 to 1 s, the pressure difference (*PD*) between the inlet and outlet increased from 0 to 100 Pa gradually, and from 1 s to 1.5 s, *PD* remained at 100 Pa. The same amount of boundary load was exerted on the solid boundaries around

the inlet, with the in-situ stress as the reference point. At the outlets, the relative pressure was set to be 0. The rest solid boundaries were set as rollers. According to the complex geometries of all models, free triangular mesh has been applied to fit in “corners” and “tips”. Boundary layer mesh has also been added to simulate the “no-slip” condition.

### *3.4 Modelling Scenarios*

In this study, several production parameters were examined, including the maximum differential injection pressure (*PD*) which represents the production pressure drawdown in the near wellbore region (80 Pa ≤ *PD* ≤ 110 Pa) (Kissell and Iannacchione 2014), temperature (*T*) (16 °C ≤ *T* ≤ 22 °C) and coal fines properties involving Young’s modulus (*E*) (4.6 GPa ≤ *E* ≤ 6.4 GPa) and strength (*S*) (80 Pa ≤ *S* ≤ 110 Pa) to investigate the impact of each parameter on coal fines generation. It should be noted that in the field, fracture pressure difference is measured on the basis straight line distance between two points, *PD* is set to be the same for each model because of the same domain size. During the modelling, only one parameter was varied at a time, while keeping others unchanged. The base case for all models was defined as *PD*=100 Pa, *T*=20 °C, *E*=5.8 GPa and *S*=100 Pa.

## 4 Results and Discussion

### *4.1 Impact of Production Pressure Drawdown*

The *PD* was varied on the range of 80 Pa ≤ *PD* ≤ 110 Pa to investigate the effect of production pressure drawdown on coal fines production. The results at steady state for different values for *PD* were compared with the base case for each model, as shown in Fig. 2, Fig. 3, Fig. 4 and Fig. 5. Red colour represents failed regions, while blue colour denotes the areas that stress is less than strength in the solid parts. To better visualize the failures in Models 3 and 4, typical failed regions were highlighted and enlarged.

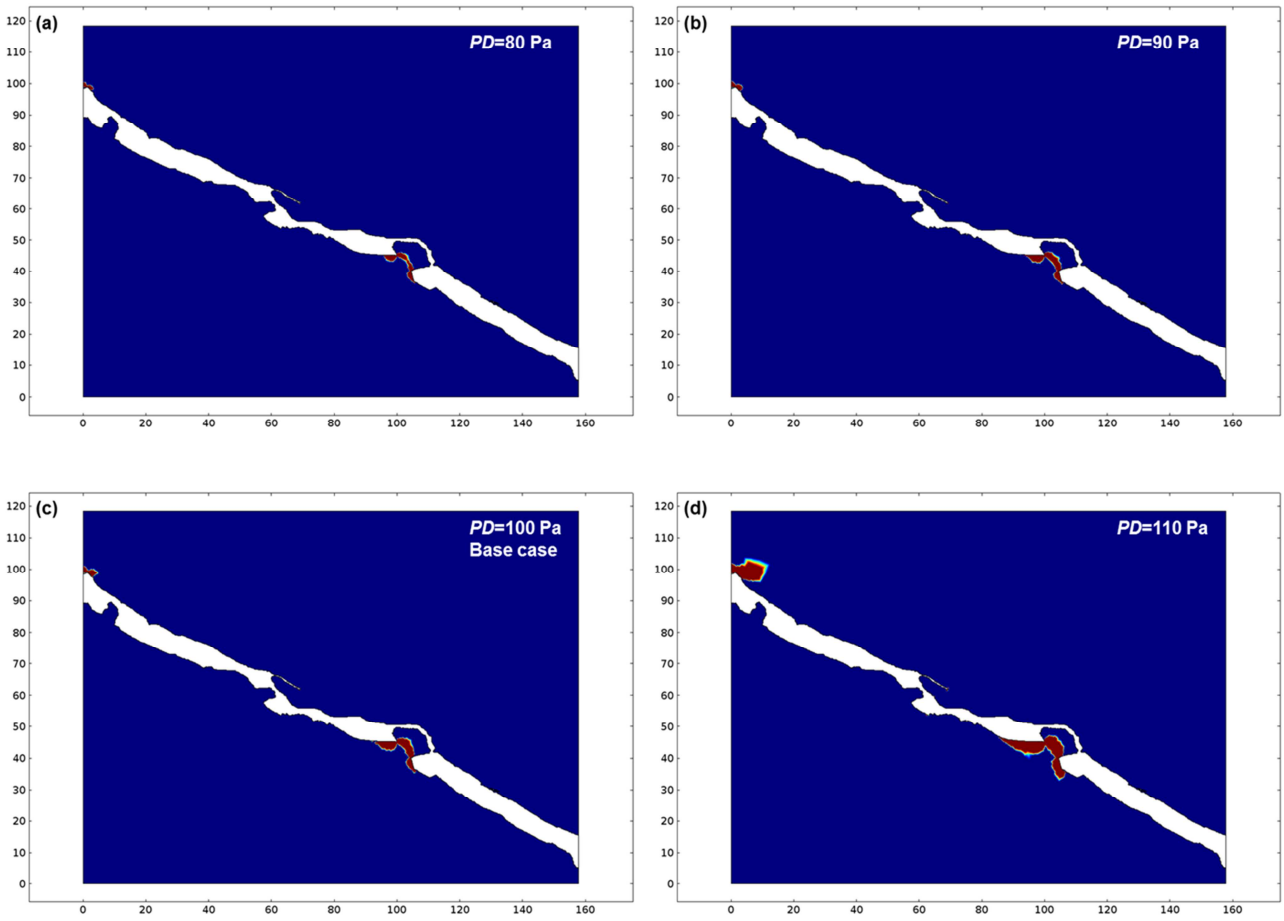


**Fig. 2.** Failure zones (red) at different values of pressure difference for Model 1 (coordinate unit: μm).

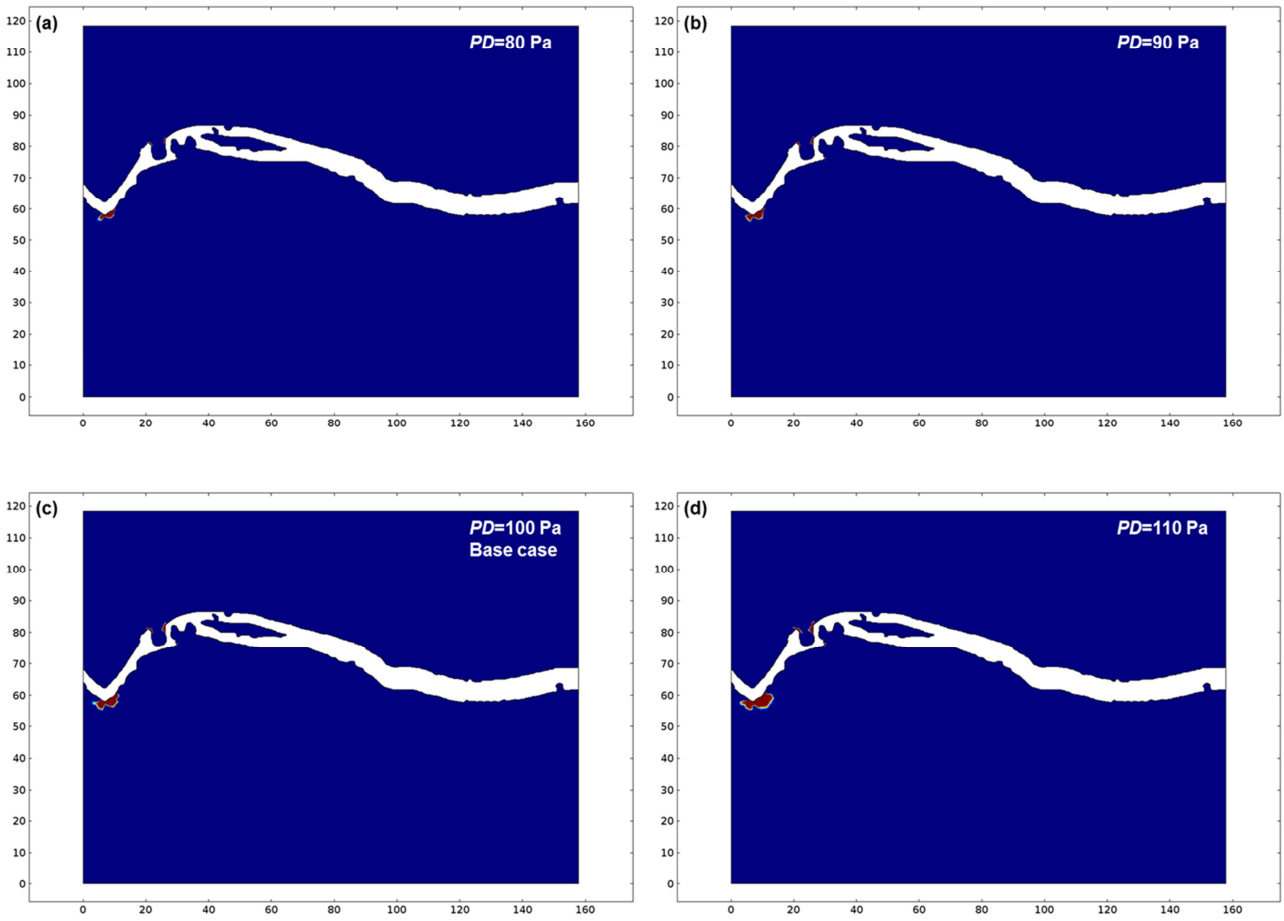


**Fig. 3.** Failure zones (red) at different values of pressure difference for Model 2 (coordinate unit: μm).

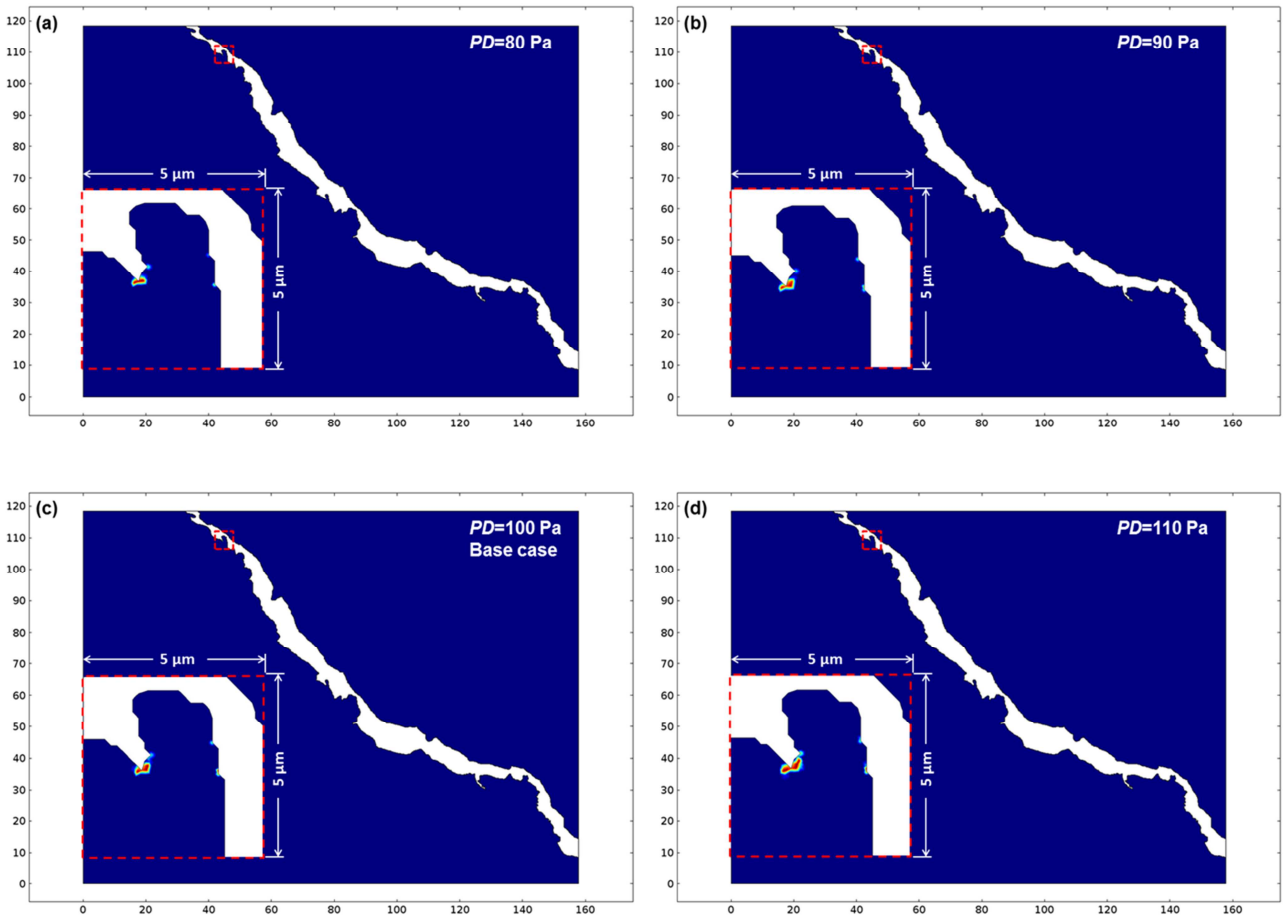


**Fig. 4.** Failure zones (red) of solid parts, and one typical highlighted failure region (red) at different values of pressure difference for Model 3 (coordinate unit: μm).

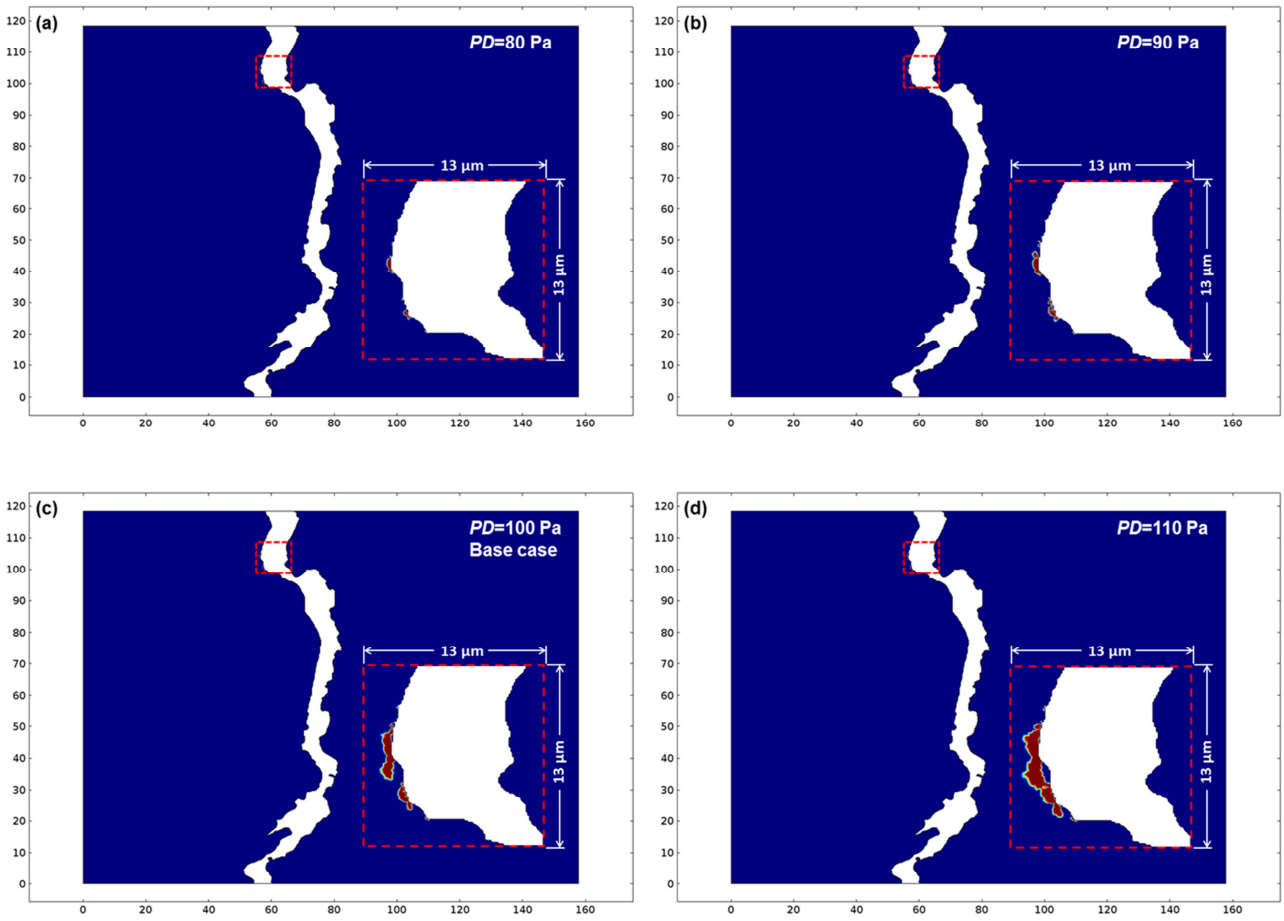


**Fig. 5.** Failure zones (red) of solid parts, and one typical highlighted failure region (red) at different values of pressure difference for Model 4 (coordinate unit: μm).

Observations on these numerical studies indicate that there are several kinds of microstructure that tend to produce coal fines. The first one includes exposed microstructures and sharp change of cleat aperture. According to Equation (9), this is because such structures narrow the cleat aperture, and the pressure drop at aperture contractions exerts high pressure gradient across these microstructures, causing high pressure force. In addition, narrowed conduit increases flow velocity, and due to the inertial effects of water flow, drastic velocity declination of water flow induces high viscous force on exposed microstructures. However, if convex microstructures are thick and/or short, pressure gradient before and after these particles is low, and/or the velocity alteration is small, the total force may not be sufficient to break them. It is the similar case for exposed microstructures which stand behind other convex particles in a close distance. The second kind refers to the regions of channel elbow. Abrupt change in flow direction applies high velocity gradient change, which boosts the viscous force in the elbow areas. The third category is the tips of dead-end micro fractures. Huge viscous force is brought about at fracture tips to cease water flowing, competing with the water flow inertial force. Nevertheless,

the viscous force can be drawn down by the variation between the flow direction and the micro fracture extension direction.

It also can be seen that, once a certain region is failed, the failure area expands with growing *PD*. The enlargement of the failure area follows certain routines for different microstructures. This can be explained by the stress concentration theory (Pilkey 2004). For example, failed zones appear first at bottom corners of an exposed particle, and then tend to connect at the bottom of such particle and become a bend, following the path with highest pressure gradient. Then the connected bend is thickened as *PD* goes further up. With regard to sharp direction change and micro crack tip areas, failure starts at the turning point of flow channel and the fracture tip, and grows with higher *PD*.

Two types of potential coal fines generation were observed in the results. One is a microstructure exhibiting connected failed regions and thus, in this case, the fine particle is entirely removed following the boundary of the connected damage bend. The other refers to the structures experiencing failure at the bottom corners. Such parts were also regarded as potential fines because the water flow is flushing them continuously, which forced the failed areas to propagate, and finally interconnected to each other and caused detachment from coal cleats. To predict the production of coal fines (*V*), the summation of these two types of failure was calculated. Considering unit thickness of the whole domain as 1 μm, for the four models, the estimated produced coal fines volumes as a function of *PD* are demonstrated in Fig. 6.

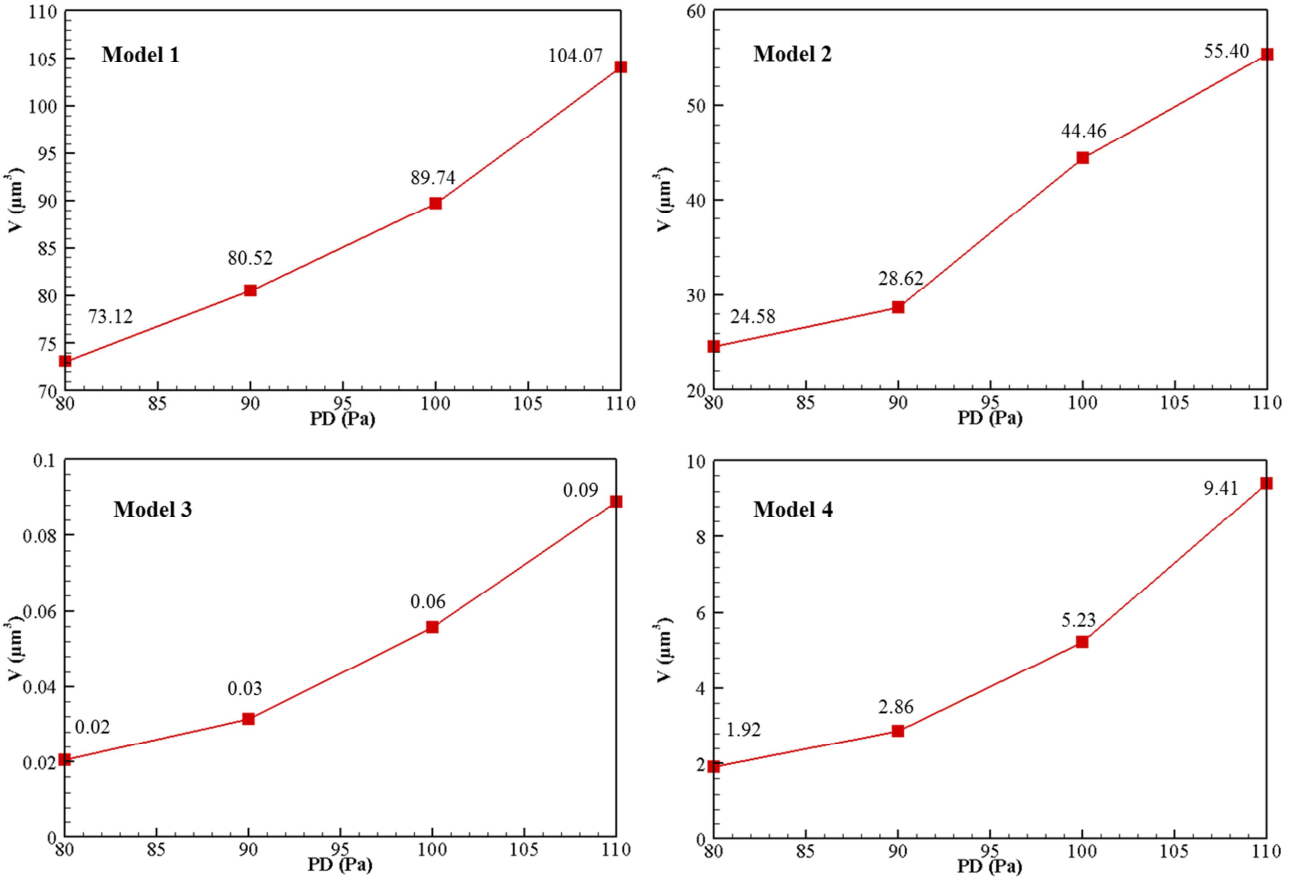


**Fig. 6.** Relationships between coal fines production and pressure difference for four models.

For this coal sample and within these *PD* frames, more coal fines are generated with increasing *PD*. This is because higher pressure induces larger pressure force, and the viscous force is also enlarged since higher velocity is imposed by higher pressure gradient. Therefore, the total force exerted on solid is larger, and more failed area can be observed. It also can be seen that *V* is more sensitive to *PD* when *PD* is in a higher value. For Model 2 specifically, a threshold value for *PD* can be noticed between 90 Pa and 100 Pa. Above this threshold *V* increases remarkably because a further detachment of coal particles take place. In the light of this statement, coal fines creation can be controlled to some extent if the production pressure drawdown is set below these thresholds by regulating the water level in the well and the dewatering pump pressure.

### *4.2 Impact of Temperature*

In order to investigate the impact of *T* on coal fines output amount, *T* was varied from 16 °C to 22 °C for each model. The results show that no evident impact of *T* on coal fine creation was observed within

studied *T* range. However, there is a linear increase of the mean flow velocity (*u*) with increasing *T*. The normalized relationships with the base case of each model between *u* and *T* are demonstrated in Fig. 7. This is because higher *T* causes lower water dynamic viscosity and density (Kestin et al. 1978) which in turn accelerate the flow. In the light of this statement, higher velocity and lower dynamic viscosity become counterparts in determining the total force acted on microstructures. As a result, the impact of *T* is so small that can be neglected in this work. It can be suggested that by increasing the temperature via reservoir management system, the dewatering process can be accelerated without producing more fines.

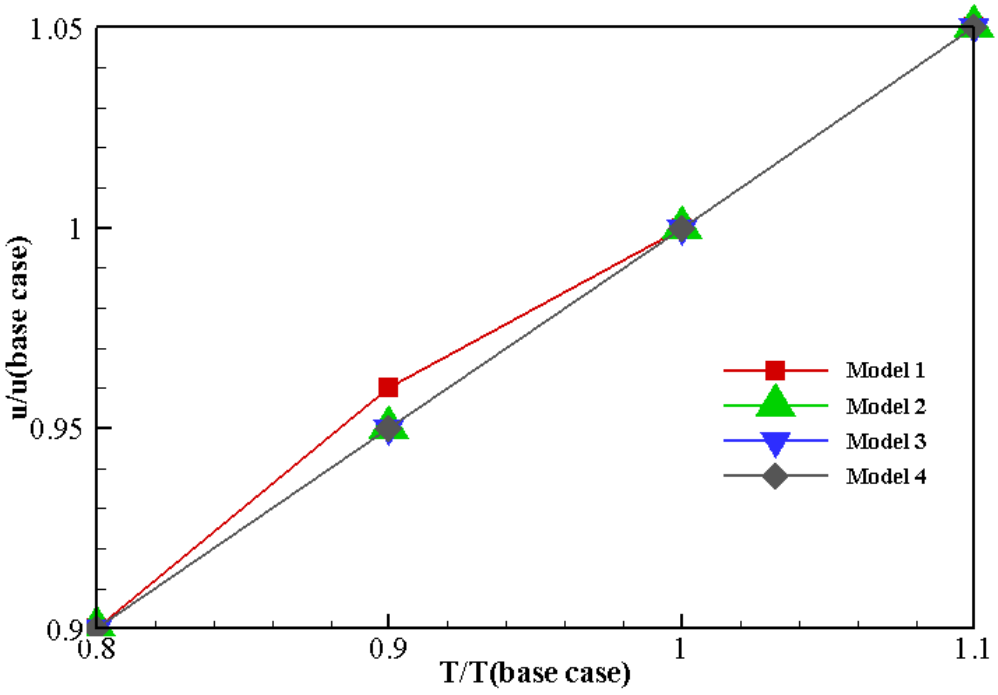


**Fig. 7.** Normalized relationships of mean velocity and temperature for four models.

*4.3 Impact of Coal Mechanical Properties*

Coal mechanical properties could also play a significant role in coal fines production. In this part, the *E* values ranging from 4.6 GPa to 6.4 GPa, and the *S* values ranging from 80 Pa to 110 Pa were changed separately to examine their corresponding effects on *V*.

Results reveal that *E* exerts little influence on *V*. It is because E value is quite high, the displacement of the solid parts is too little to distinguish the variation of E, which does not influence the flow behaviour. With respect to *S*, the simulation results are displayed in Fig. 8, Fig. 9, Fig. 10 and Fig. 11. Failed area

is shrinking as *S* is growing. The suspect coal fines region and failure propagation mode are similar with those of changing *PD*. However, the failed area is larger compared with that of corresponding *PD* value, which represents that *V* is more sensitive to *S* rather than *PD*.

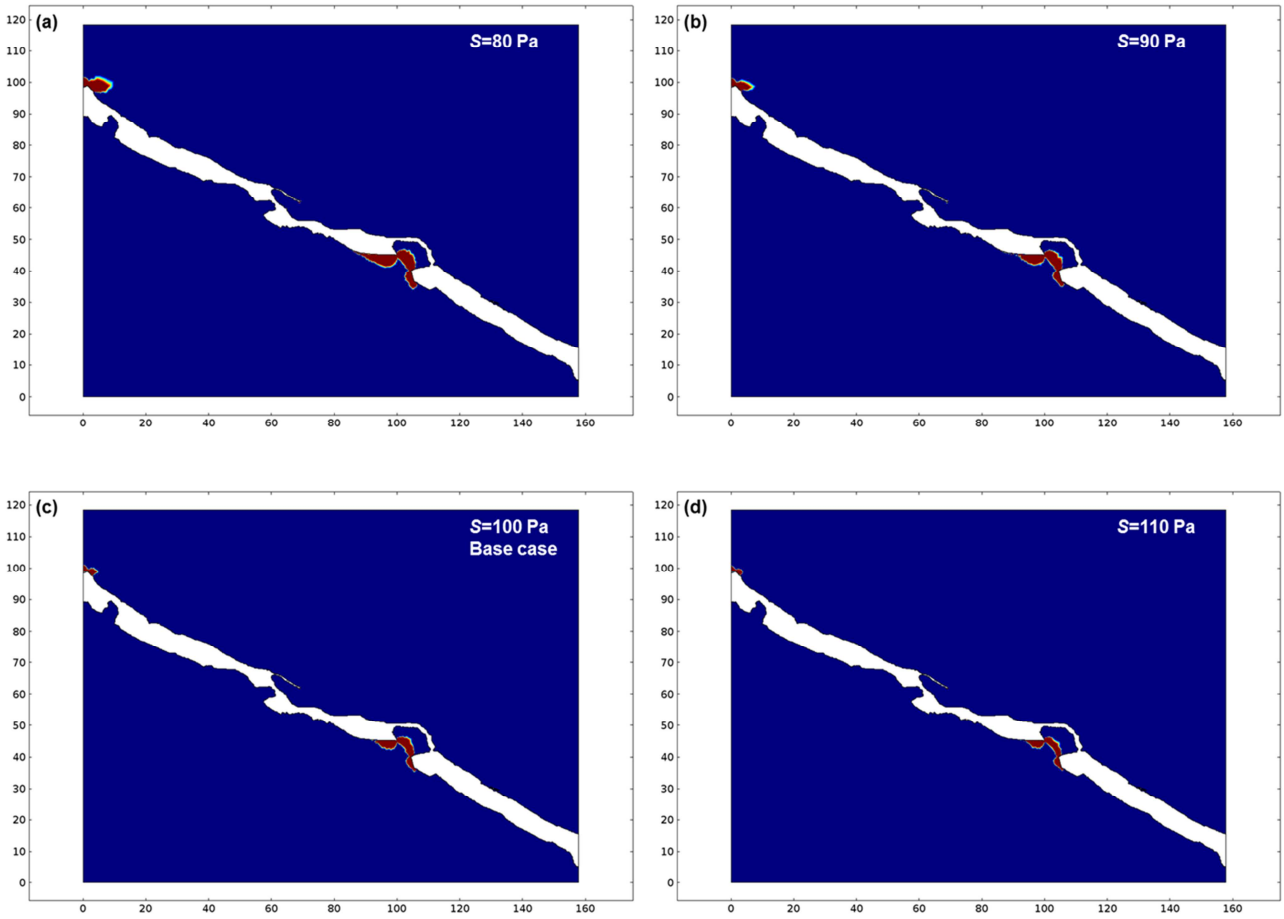


**Fig. 8.** Failure zones with varying strength for Model 1 (coordinate unit: μm).

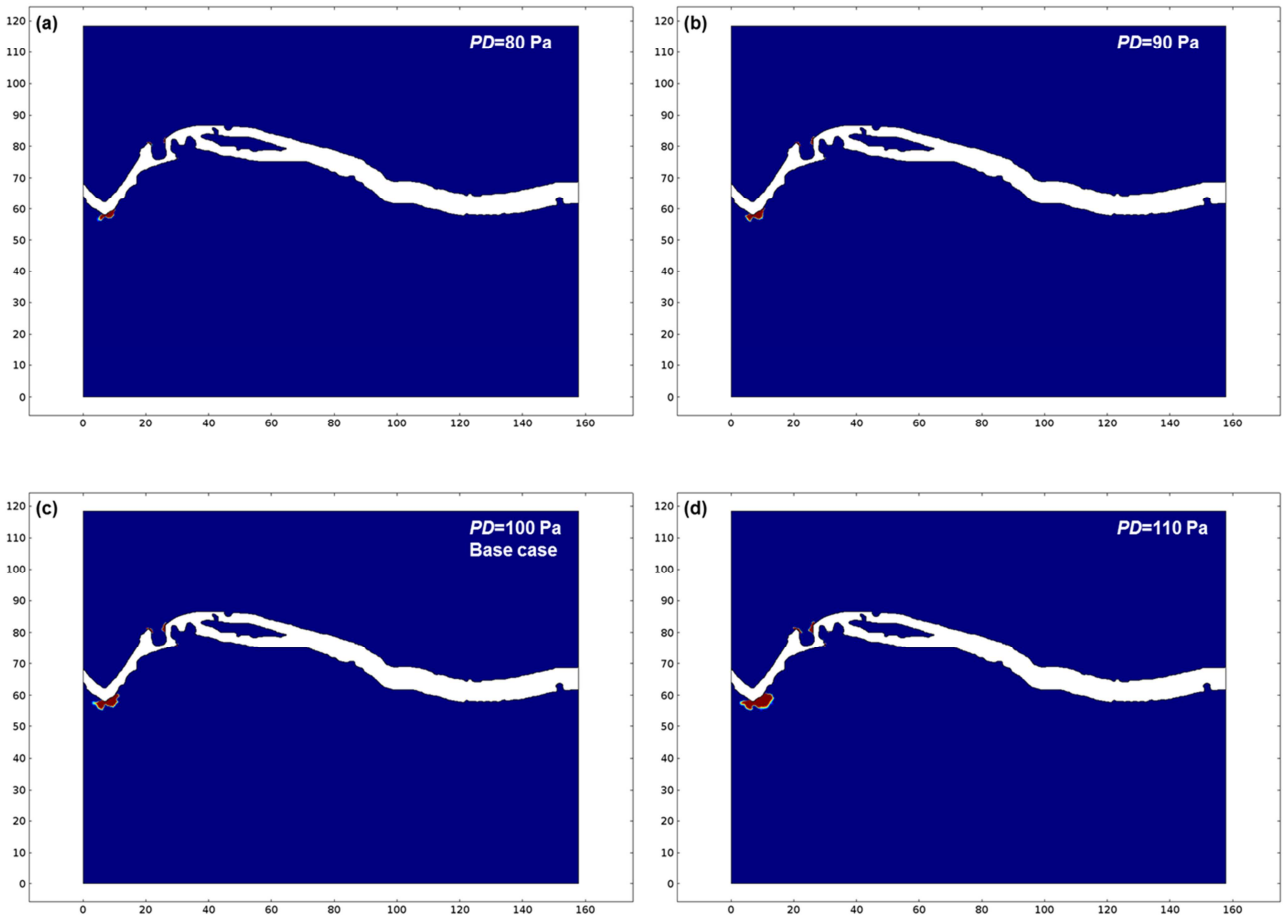


**Fig. 9.** Failure zones with varying strength for Model 2 (coordinate unit: μm).

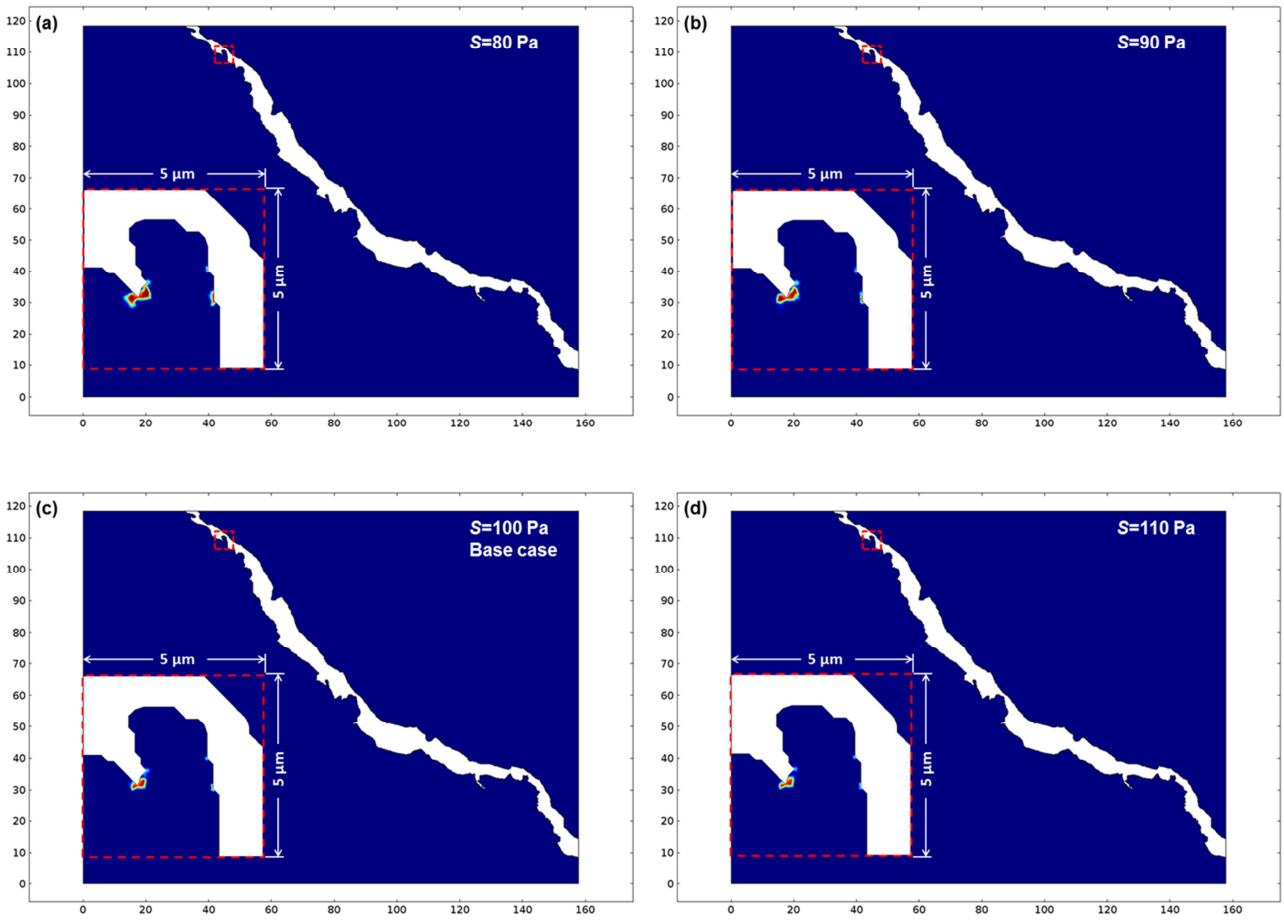


**Fig. 10.** Failure zones (red) of solid parts, and one typical highlighted failure region (red) at different values of strength for Model 3 (coordinate unit: μm).

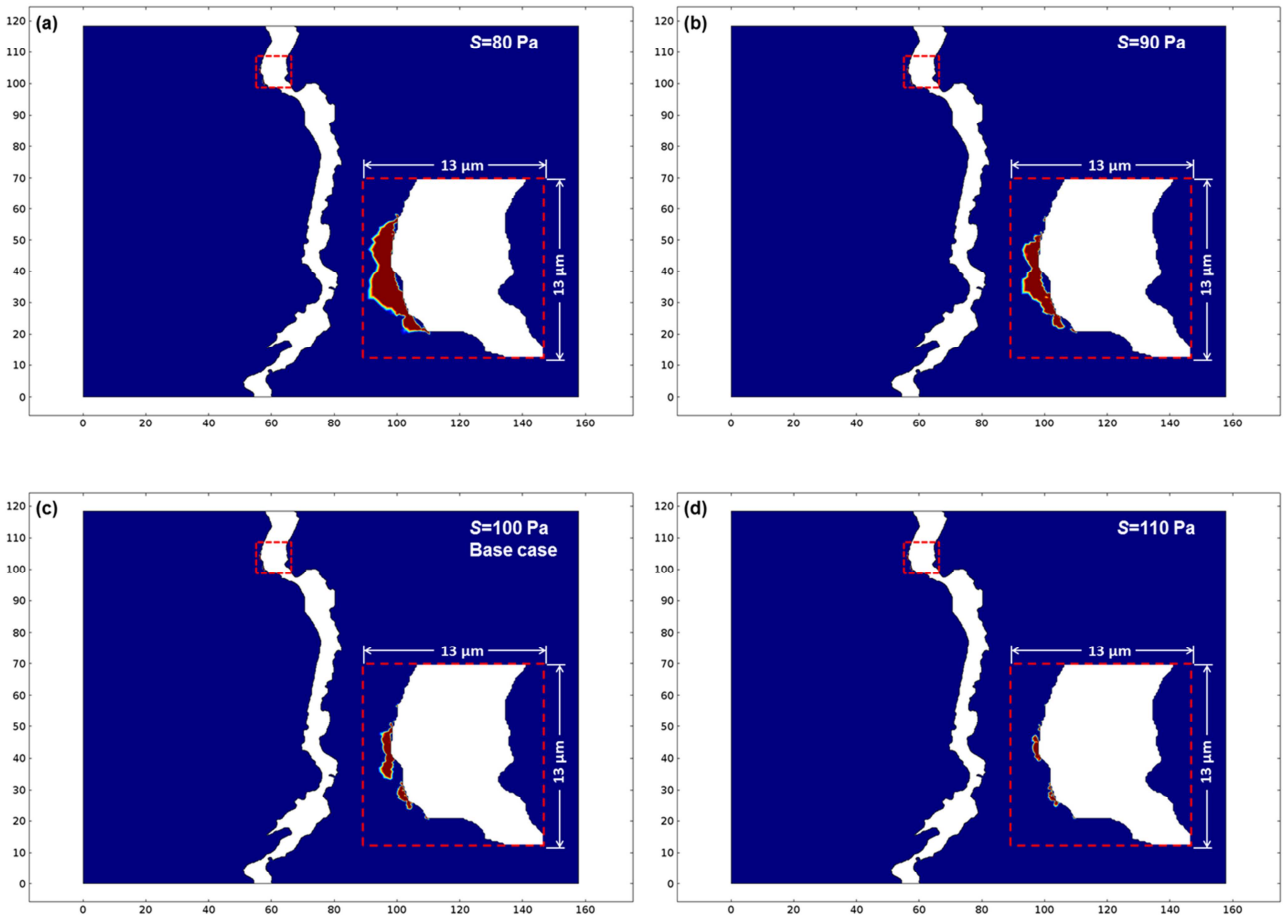


**Fig. 11.** Failure zones (red) of solid parts, and one typical highlighted failure region (red) at different values of strength for Model 4 (coordinate unit: μm).

For the four models, *V* values are plotted against different *S* (Fig. 12). *V* is dragged down by increasing *S*, and it is more sensitive to *S* when *S* is rather low. Such relationships indicate that more coal fines production could be expected from soft and weak coal seams, which is a potential risk that should be considered when designing the production strategy. This is in good consistency with previous finding (Cao et al. 2012). Therefore, coal fines output can be better controlled if production takes place in coal layers with hard physical property.

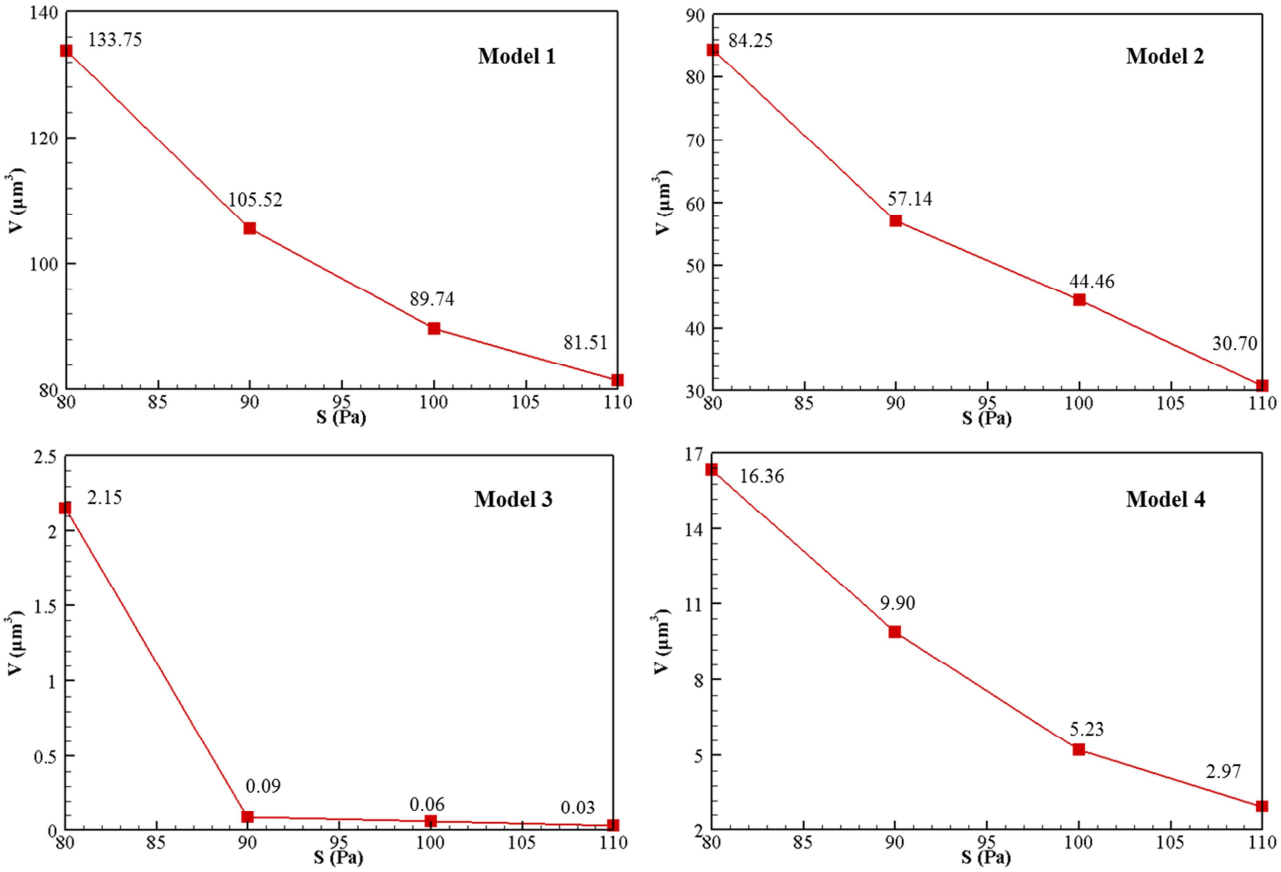


**Fig. 12.** Relationships between coal fines production and strength for four models.

### *4.4 Impact of Cleat Geometry*

In order to examine how cleat geometry affects coal fines generation, the average pressure gradient in each cleat must be the same. Therefore, the effective flow length ($l$) and the mean cleat aperture ($a$) were computed. The $l$ was defined as the average length of cleat surfaces; while the $a$ was defined as arithmetic mean aperture of a cleat. *PD* was kept as 100 Pa for Model 1 to develop *PD*s for the rest models. The corresponding values for each model are listed in Table 2. Other parameters except for *PD* were kept as the ones in the base cases.

**Table 2** Effective flow length, mean cleat aperture and pressure difference for each model

| Model Number | $l$ (μm) | $a$ (μm) | *PD* (Pa) |
|---|---|---|---|
| 1 | 241.05 | 4.157 | 100.00 |
| 2 | 200.60 | 4.969 | 83.22 |
| 3 | 220.55 | 3.756 | 91.50 |

| | | | |
|---|---|---|---|
| 4 | 178.15 | 4.770 | 73.91 |

The flow velocity contours for each model are plotted with the same colour scale ranging from 0 to 0.002 m/s in Fig. 13. Flow velocities in Models 2 and 4 are higher than those in Models 1 and 3, because the mean cleat apertures are larger for Models 2 and 4. The flow boundary condition was set to be no-slip at walls, which means the velocity at cleat surface is 0. In this manner, bigger aperture has less fraction of influenced zones induced by no-slip condition, and has higher flow velocity.

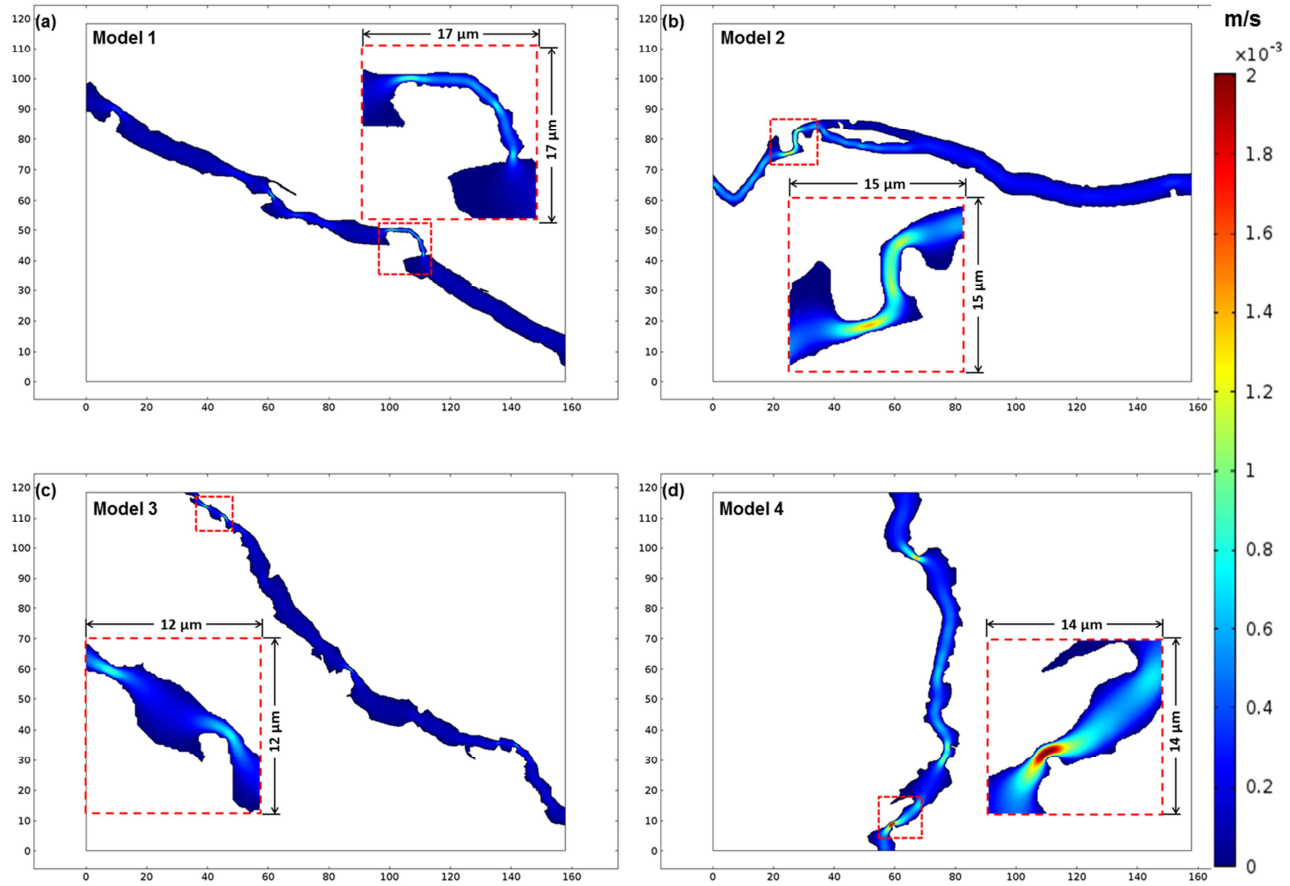


**Fig. 13.** Flow velocity contours and highlighted regions showing highest velocity in each model (coordinate unit: μm).

The evolutions of the failed area for four models were calculated. It is noted that coal fines are not generated until *PD* reaches critical values. When *PD* exceeds these critical values, failed zones start to expand rapidly. The critical values are listed in Table 3, showing little variance according to different cleat geometries. The indication of the critical pressures is that during the dewatering process, if the pressure difference between reservoir pressure and bottom-hole pressure (BHP) can be controlled below the critical value through BHP management system, coal fines generation can be contained at a minimum level.

**Table 3** Critical pressure difference values for four models

| Model Number | Time (s) | Critical *PD* (Pa) |
|---|---|---|
| 1 | 0.41 | 34.12 |
| 2 | 0.44 | 32.46 |
| 3 | 0.40 | 29.28 |
| 4 | 0.45 | 30.30 |

The relationship between *u* and *a* shows a general positive fashion (Fig. 14). The higher value for *u* in Model 4 compared to that in Model 2 can be explained as the flow branch brings up the proportion of no-slip influenced zones in Model 2. *V* seems to be irrelevant to *a*, this is probably because *V* is closely related to the local flow velocity distribution rather than the mean velocity, and the local microstructures as described previously. The indication is that the production wellbore and fracturing should be located away from disturbed coal seams, because they may have rougher cleats to generate more coal fines.

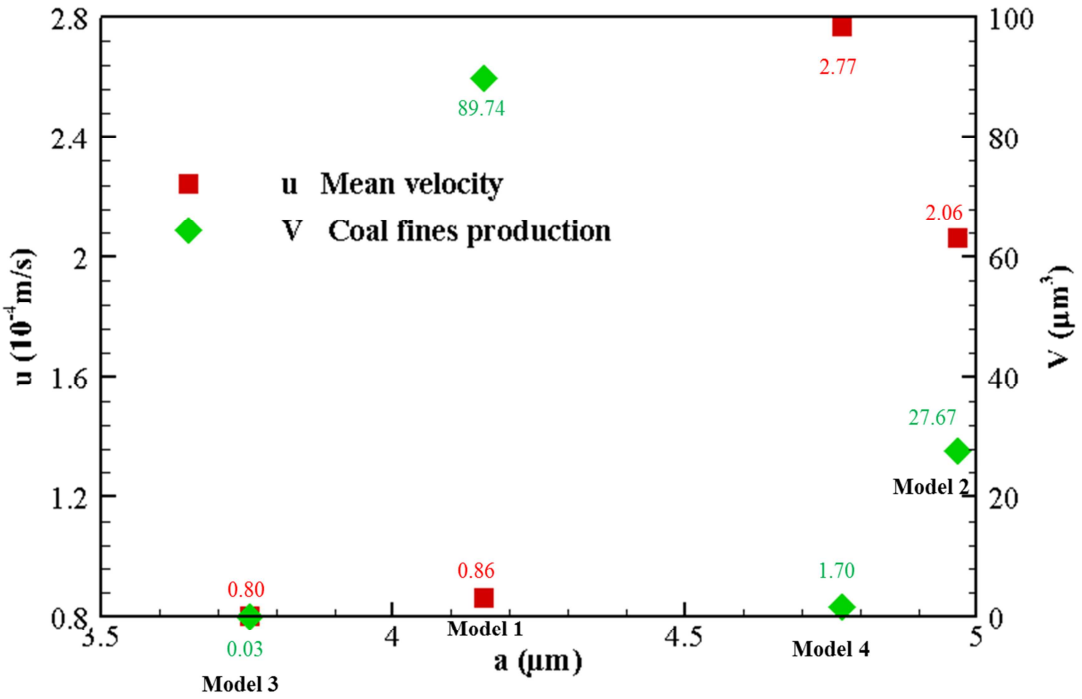


**Fig. 14.** Mean velocity and coal fines production as a function of average aperture with the same average pressure gradient.

## 5 Conclusions

In this study, identification of the surface properties of coal cleats was conducted using the Scanning Electron Microscopy (SEM) images corresponding to a coal sample from Bulli Seam of Sydney Basin in Australia. Four SEM images were then analysed to obtain the actual cleat geometries and the characteristics of coal fines distribution. A fully coupled numerical model was developed to identify the creation process of coal fines at a micro-scale. The impacts of production conditions on coal fines generation were comprehensively studied. The below conclusions are drawn:

1. The results show that for this coal sample, the size distributions of coal fines are in the order of hundreds of nanometres to several microns.
2. A critical pressure difference was found for each model, above which coal fines begin to yield rapidly. Such critical pressure seems to be irrelevant to cleat geometry. It was also found that more fines are generated with increasing pressure, and threshold values dependent on cleat geometry exist, above which coal fines production grows dramatically. However, little variance was observed on coal fines generation with changing temperature and Young's modulus.
3. The mean flow velocity is accelerated by temperature build up without producing more coal fines. Water flows faster in wider cleats under the same cleat pressure gradient.
4. Strength plays a significant role in determining the amount of coal fines. Coal fines are generated less with increasing strength, and coal fines production is more sensitive to strength variations at rather low level. Moreover, strength exerts more effects on coal fines generation than pressure.
5. Coal fines production is strongly related to coal cleat geometry and local flow velocity distribution. Observations show that exposed microstructures, cleat elbow regions and micro fracture tips are more likely to become coal fines. These findings can provide useful insight to the production control under different conditions to mitigate the coal fines issue for coalbed methane production.

## 6 Acknowledgements

This work was partially supported by new staff start-up from the University of Queensland, UWA-UQ Bilateral Research Collaboration Award (2013002812), ARC Discovery Project (DP150103467), MEA Research Grant and the State Key Laboratory for GeoMechanics and Deep Underground Engineering,

China University of Mining & Technology (Grant No.: SKLGDUEK1302). These sources of support are gratefully acknowledged.

**References**

Bedrikovetsky, P.G., Vaz, A., Jr., Machado, F.A., Zeinijahromi, A., and Borazjani, S. 2011. "Well Productivity Decline due to Fines Migration and Production: (Analytical model for the regime of strained particles accumulation)."

Black, D.J. 2011. "Factors affecting the drainage of gas from coal and methods to improve drainage effectiveness." PhD, School of Civil, Mining and Environmental Engineering, University of Wollongong.

Cao, L., Zhang, S., Shi, H., Bai, J., Wang, H., and Zhu, W. 2012. "Coal dust migration and treatment for coalbed methane horizontal wells in Qinshui Basin." *Oil Drilling & Production Technology* 34 (4):3.

Chen, Z., Wang, Y., and Sun, P. 2009. "Destructive influences and effective treatments of coal powder to high rank coalbed methane production." *Journal of China Coal Society* 34 (2):229-232.

Civan, F. 2007. "Particulate processes in porous media." In *Reservior formation damage*, edited by Faruk Civan, 191-234. Elsevier.

Fan, Y., Dong, X., and Li, H. 2015. "Dewatering effect of fine coal slurry and filter cake structure based on particle characteristics." *Vacuum* 114 (0):54-57. doi: http://dx.doi.org/10.1016/j.vacuum.2015.01.003.

Greenhalgh, S.A., and Emerson, D.W. 1986. "Elastic properties of coal measure rocks from the Sydney Basin, New South Wales." *Exploration Geophysics* 17 (3):157. doi: 10.1071/EG986157.

Hibbeler, J., Garcia, T., and Chavez, N. 2003. "An Integrated Long-Term Solution for Migratory Fines Damage."

Hou, S., Wang, X., Wu, M., Wang, X., Jing, Z., and Aiwe, Z. 2014. "Coal fines production in different drainage stages and its influence on productivity." In *Progress in Mine Safety Science and Engineering II*, 1253-1257. CRC Press.

Huang, T., Crews, J.B., Gabrysch, A.D., and Jeffrey, R.M. 2012. Controlling coal fines in coal bed operations. Google Patents.

Kestin, J., Sokolov, M., and Wakeham, W.A. 1978. "Viscosity of liquid water in the range −8 °C to 150 °C." *Journal of Physical and Chemical Reference Data* 7 (3):941. doi: 10.1063/1.555581.

Khilar, K.C., and Fogler, H.S. 1998. *Fines migration in porous media*: Kluwer Academic Publishers.

Kissell, F.N., and Iannacchione, A.T. 2014. "Gas outbursts in coal seams." In *Coal bed methane from prospect to pipeline*, edited by Pramod Thakur, Steve Schatzel and Kashy Aminian. Elsevier.

Koyama, T., Neretnieks, I., and Jing, L. 2008. "A numerical study on differences in using Navier–Stokes and Reynolds equations for modeling the fluid flow and particle transport in single rock

fractures with shear." *International Journal of Rock Mechanics and Mining Sciences* 45 (7):1082-1101. doi: http://dx.doi.org/10.1016/j.ijrmms.2007.11.006.

Kumar, D. 2008. "Investigation into floor bearing strength of Indian coal measure strata by finite element modeling." 6th international symposium on ground support in mining & civil engineering, Cape Town.

Kundu, P., Cohen, I., and Dowling, D. 2011. *Fluid mechanics*: Elsevier.

Lagasca, J.R.P., and Kovscek, A.R. 2014. "Fines migration and compaction in diatomaceous rocks." *Journal of Petroleum Science and Engineering* 122 (0):108-118. doi: http://dx.doi.org/10.1016/j.petrol.2014.06.024.

Li, Y., Wang, L., Liu, G., Yan, L., and Zou, Z. 2010. "Study on coal reservoir damage mechanism in dewatering and extraction process of CBM wells." *China Coalbed Methane* 7 (6):39-47.

Liu, Q., Cheng, Y., Zhou, H., and Guo, P. 2014. "A Mathematical Model of Coupled Gas Flow and Coal Deformation with Gas Diffusion and Klinkenberg Effects." *Rock mechanics and rock engineering*.

Liu, S., Zhang, X., Yuan, W., and Tian, X. 2012. "Regularity of coal powder production and concentration control method during CBM well drainage." *Journal of China Coal Society* 37:412-415.

Magill, D.P., Ramurthy, M., Jordan, R., and Nguyen, P.D. 2010. "Controlling Coal-Fines Production in Massively Cavitated Openhole Coalbed-Methane Wells."

Marcinew, R.P., and Hinkel, J.J. 1990. "Coal Fines-Origin, Effects and Methods to Control Associated Damage." Alberta.

Massarotto, P., Iyer, R.S., Elma, M., and Nicholson, T. 2013. "An Experimental Study on Characterizing Coal Bed Methane (CBM) Fines Production and Migration of Mineral Matter in Coal Beds." *Energy & Fuels* 28 (2):766-773. doi: 10.1021/ef401098h.

Miranda, R.M., and Underdown, D.R. 1993. "Laboratory Measurement of Critical Rate: A Novel Approach for Quantifying Fines Migration Problems."

Mirshekari, B., Dadvar, M., Modarress, H., and Dabir, B. 2013. "Modelling and simulation of multiphase flow formation damage by fine migration including the multilayer deposition effect." *International journal of oil gas and coal technology* 6 (6):624-644. doi: 10.1504/IJOGCT.2013.056711.

Mises, R.v. 1913. "Mechanik der festen Körper im plastisch deformablen Zustand." *Nachrichten von der Gesellschaft der Wissenschaften zu Göttingen*:582-592.

Muecke, T.W. 1979. "Formation Fines and Factors Controlling Their Movement in Porous Media."

*Journal of Petroleum Technology* 31 (2):144-150.

Narah, D. 2007. "Hydraulic fracturing of coalseams." In *Coalbed methane: principles and practices*.

Nguyen, P.D., Vasquez, J.E., Weaver, J.D., and Welton, T.D. 2010. "Maintain well productivity through inhibiting scale formation and controlling fines migration." SPE Asia Pacific Oil & Gas Conference and Exhibition, Brisbane.

Okotie, V.U., and Moore, R.L. 2010. "Well Production Challenges and Solutions in a Mature, Very Low-Pressure Coalbed Methane Reservoir." SPE Annual Technical Conference and Exhibition, Florence.

Palmer, I.D., Moschovidis, Z.A., and Cameron, J.R. 2005. "Coal Failure and Consequences for Coalbed Methane Wells." SPE Annual Technical Conference and Exhibition, Dallas, Texas.

Pilkey, W.D. 2004. *Formulas for stress, strain, and structural matrices*. 2 ed: Wiley.

Qiu, K., Gherryo, Y., Shatwan, M., Fuller, J., and Martin, W. 2008. "Fines migration evaluation in a mature field in Libya." Asia Pacific Oil & Gas Conference and Exhibition, Perth.

Turner, L.G., Steel, K.M., and Pell, S. 2013. "Novel Chemical Stimulation Techniques to Enhance Coal Permeability for Coal Seam Gas Extraction."

Varnes, D.J. 1962. Analysis of plastic deformation according to Von Mises' theory, with application to the South Silverton area, San Juan County, Colorado. edited by U.S. Geological Survey: U.S. Govt. Print. Off.

Vermeltfoort, A.T., and Schijndel, A.W.M.V. 2013. "Comsol simulations of cracking in point loaded masonry with randomly distributed material properties." COMSOL conference, Boston.

Wang, H., and Lan, W. 2012. "Discussion on formation mechanism of coal powder in coalbed methane well." *China Coal* 2:95-105.

Wang, H., Lan, W., Liu, Y., Zhang, H., and Yu, H. 2013. "Mathematical model of fluid-solid coupling percolation with coal powder in coal reservoir." *Natural Gas Geoscience* 24 (4):667-670.

Wei, C., Zou, M., Sun, Y., Cai, Z., and Qi, Y. 2015. "Experimental and applied analyses of particle migration in fractures of coalbed methane reservoirs." *Journal of Natural Gas Science and Engineering* 23 (0):399-406. doi: http://dx.doi.org/10.1016/j.jngse.2015.02.022.

Wei, Y., Cao, D., Yuan, Y., Zhu, X., Yao, Z., and Zhou, J. 2013. "Characteristics and controlling factors of pulverized coal during coalbed methane drainage in Hancheng area." *Journal of China Coal Society* 38 (8):1424-1429.

Zeinijahromi, A., Machado, F.A., and Bedrikovetsky, P.G. 2011. "Modified Mathematical Model for Fines Migration in Oil Fields."

Zhang, G., Tian, W., Tao, S., Bai, J., Shi, H., and Cheng, H. 2011. "Experimental research of coal grain

migration rules of coalbed methane." *Journal of Oil and Gas Technology* 33 (9):105-108.

Zhu, H.Q., Zhu, S.H., Jia, G.W., and Song, Z.Y. 2014. "Numerical simulation of blasting effects on soft coal under different confining pressure." In *Progress in Mine Safety Science and Engineering II*, 997-1002. CRC Press.

Zou, Y.S., Zhang, S.C., and Zhang, J. 2014. "Experimental Method to Simulate Coal Fines Migration and Coal Fines Aggregation Prevention in the Hydraulic Fracture." *Transport in Porous Media* 101 (1):17-34. doi: 10.1007/s11242-013-0228-9.

- Quantification of coal fines generation using numerical modelling for the first time
- The effects of production parameters on coal fines generation are investigated and compared
- The importance of cleat microstructures on coal fines production is examined
- Identification of coal fines based on real coal cleat images is performed